PHYSICAL REVIEW B **92**, 125103 (2015)

Shear viscosity of strongly interacting fermionic quantum fluids

Nandan Pakhira and Ross H. McKenzie*
School of Mathematics and Physics, The University of Queensland, Brisbane, QLD 4072, Australia
(Received 3 June 2015; revised manuscript received 17 August 2015; published 1 September 2015)

Eighty years ago, Eyring proposed that the shear viscosity of a liquid η has a quantum limit $\eta \gtrsim n\hbar$ where n is the density of the fluid. Using holographic duality and the anti–de Sitter/conformal field theory correspondence in string theory, Kovtun, Son, and Starinets (KSS) conjectured a universal bound $\frac{\eta}{s} \geqslant \frac{\hbar}{4\pi k_B}$ for the ratio between the shear viscosity and the entropy density s. Using dynamical mean-field theory, we calculate the shear viscosity and entropy density for a fermionic fluid described by a single-band Hubbard model at half-filling. Our calculated shear viscosity as a function of temperature is compared with experimental data for liquid ^{3}He. At low temperature, the shear viscosity is found to be well above the quantum limit and is proportional to the characteristic Fermi liquid $1/T^2$ dependence, where T is the temperature. With increasing temperature and interaction strength U, there is significant deviation from the Fermi liquid form. Also, the shear viscosity violates the quantum limit near the crossover from coherent quasiparticle-based transport to incoherent transport (the bad metal regime). Finally, the ratio of the shear viscosity to the entropy density is found to be comparable to the KSS bound for parameters appropriate to liquid ^{3}He. However, this bound is found to be strongly violated in the bad metal regime for parameters appropriate to lattice electronic systems such as organic charge-transfer salts.

DOI: 10.1103/PhysRevB.92.125103 PACS number(s): 71.27.+a, 05.60.Gg, 67.10.Jn

I. INTRODUCTION

The viscosity of a fluid is a measure of its resistance to externally applied *shear* or *tensile stress*. The shear viscosity of a fluid measures the resistance of a fluid to *shear flows*, where adjacent layers of a fluid move parallel to each other but with different speeds. The differential speed between different layers will give rise to friction between different layers which will resist their relative motion. This is known as the *viscous drag*. For example, the viscous drag force per unit area in the x direction τ_{xy} due to velocity gradient $\partial u_x(y)/\partial y$ in the perpendicular y direction is given by

$$\tau_{xy} = -\eta \frac{\partial u_x(y)}{\partial y}, \tag{1}$$

where η is the coefficient of shear viscosity. The SI unit of shear viscosity is Pascal-seconds (Pa · s) equivalent to *Newton-second per square meter* (N · s m^{-2}). The shear viscosity of water is about 10^{-3} (Pa · s) at room temperature whereas the shear viscosity of highly viscous fluids such as glasses near the glass transition temperature can be as large at 10^{13} Pa · s.

For fluids η can be measured through Stokes law for sound attenuation [1]:

$$\alpha = \frac{2\omega^2\eta}{3\rho c_s^3}, \tag{2}$$

where α is the rate of attenuation, ρ is the mass density of the fluid, ω and c_s are the frequency and velocity of sound in the medium, respectively. This equation has been used to determine the shear viscosity as a function of temperature for liquid ^{3}He (a correlated neutral fermion fluid). Extensive experimental data have been reviewed by Huang *et al.* [2].

The shear viscosity for an electron gas in metals, calculated from solution of the Boltzmann equation, is given by [3]

$$\eta = \tfrac{1}{5} n\hbar k_F \ell, \tag{3}$$

where n is the density of electrons, k_F is the Fermi velocity, and ℓ is the electronic *mean-free path*, respectively. In the quasiparticle regime of transport $k_F\ell \gg 1$, i.e., the mean-free path is much larger than the lattice spacing $a \sim k_F^{-1}$. Hence, in analogy with the Mott-Ioffe-Regel (MIR) limit, $\sigma_{\mathrm{MIR}} = \frac{e^2}{ha}$, for minimum metallic conductivity, we can conjecture a lower limit for the shear viscosity η_q:

$$\eta_q = \tfrac{1}{5} n\hbar \tag{4}$$

corresponding to the case where the electronic mean-free path becomes comparable to lattice spacing. Also, a comparable limit $\eta \gtrsim n\hbar$ was proposed by Eyring [4] almost 80 years ago. For a large class of strongly correlated systems such as $3d$ transition-metal oxide compounds, organic charge-transfer salts such as κ-(BEDT-TTF)$_2$X, the MIR limit is violated [5–7] and the coherent quasiparticle-based transport picture breaks down, i.e., $\ell < a$. Similarly, we might expect that in the incoherent regime of transport, the shear viscosity η could violate the quantum limit to coherent transport, i.e., $\eta < \eta_q$.

Recently, a string theory based approach has been proposed to understand incoherent quantum transport in strongly correlated electron systems, especially the strange metal regime of doped cuprates [8–12]. The key idea of this method is to map a strongly coupled conformal field theory (CFT) to weakly coupled gravity in the anti–de Sitter (AdS) space in higher dimension [13]. This is known as the holographic duality or AdS/CFT correspondence. Furthermore, event horizon dynamics of a black hole in the anti–de Sitter space can be mapped to the dynamics of classical fluids. Using the AdS/CFT correspondence, Kovtun, Son, and Starinets (KSS) [14] calculated the ratio η/s of the shear viscosity (η) and the entropy density (s) in a specific string theory model (type IIB)

*r.mckenzie@uq.edu.au; condensedconcepts.blogspot.com

and proposed a universal lower bound for the ratio

$$\frac{\eta}{s} \geqslant \frac{\hbar}{4\pi k_B} \tag{5}$$

in any material or field theory. This bound is found to be well respected in classical fluids such as water and quantum fluids such as the quark-gluon plasma created in the relativistic heavy ion collider (RHIC) [15], ultracold atomic Fermi gases in the unitary limit of scattering [16], and by theoretical calculations for graphene [17] and for ultracold atomic Fermi gases [18,19]. It has recently been found that for the strongly interacting Fermi gas, both experimentally [20] and theoretically [21], that the viscosity-entropy ratio is a minimum, not at unitarity, but on the BEC side, with a minimum value of $\simeq 0.2\hbar/k_B$. Possible violations of the KSS bound have been discussed for higher derivative versions of gravity and with the inclusion of massive quarks [22].

In a recent calculation we tested a related but distinct bound on charge diffusivity $D \geqslant \frac{\hbar v_F^2}{k_B T}$, where v_F is the Fermi velocity, proposed by Hartnoll [11]. We found [23] clear violation of this bound in the strong coupling (bad metal) regime of the Hubbard model. In this paper, we calculate the shear viscosity in a single-band Hubbard model and explore possible violations of the conjectured quantum bounds on η and η/s.

Overall, we find that the scale of the viscosity in a correlated band system with a lattice constant a in d dimensions is set by

$$\eta_0^b \equiv \frac{\hbar}{a^d}\left(\frac{m}{m_b}\right)^2\left[\frac{\pi}{2d(d-1)}\right], \tag{6}$$

where m is the free-fermion mass and $m_b \equiv \hbar^2/(a^2 E_b)$ is a mass scale determined by some energy scale E_b defined by the band structure, such as the half-bandwidth W or the rescaled hopping integral t^* for a hypercubic lattice. A detailed derivation of the expression in Eq. (6) will be provided in the following sections. We show that for a lattice system η_0^b is the relevant scale for the analog of the Mott-Ioffe-Regel limit. We will see that the presence of this new scale, absent in a conformally invariant system, can increase the likelihood of violation of the KSS bound.

The organization of the paper is as follows. In Sec. II, we introduce the Kubo formula for calculation of the shear viscosity using linear-response theory. In Sec. III, we briefly describe the dynamical mean-field theory (DMFT) approach for calculating properties of a single-band Hubbard model and the iterated perturbation theory (IPT) based approach used to treat the DMFT self-consistency for the associated single-impurity Anderson model. In the same section, we introduce calculation of the shear viscosity and entropy density in DMFT. In Sec. IV, we first briefly review experimental results for the temperature dependence of the shear viscosity of liquid ^{3}He and its possible description by a Hubbard model. In Sec. V, we show our results for the Hubbard model on the Bethe and hypercubic lattices at half-filling. Similar results are obtained for both lattices. We compare our calculations to experimental results for liquid ^{3}He. The temperature dependence of the ratio of the viscosity to the entropy density is calculated. It is found that in the bad metal regime near the Mott metal-insulator transition this ratio can be smaller than the KSS bound. In Sec. VI, we discuss about experimental measurement of shear viscosity in charged systems and finally we conclude in Sec. VII.

II. SHEAR VISCOSITY

Nonrelativistic simple fluids are characterized by the conserved mass density ρ, the momentum density $\boldsymbol{\pi}$, and the energy density $\mathcal{E}$. These quantities will satisfy the following conservation laws [24]:

$$\frac{\partial \rho}{\partial t} = -\boldsymbol{\nabla}\cdot\boldsymbol{\pi}, \tag{7}$$

$$\frac{\partial \pi_i}{\partial t} = -\nabla_j \Pi_{ij} \tag{8}$$

$$\frac{\partial \mathcal{E}}{\partial t} = -\boldsymbol{\nabla}\cdot\boldsymbol{j}^{\epsilon}, \tag{9}$$

where Π_{ij} is the momentum current density that the following discussion shows is central to the shear viscosity. As a consequence, in analogy with the case of Ohm's law for electrical conductivity, $j_\alpha^e = \sigma_{\alpha\beta}E_\beta \equiv -\sigma_{\alpha\beta}\partial_\beta\phi(\mathbf{r})$, the generalized Newton's law for shear flow is

$$\Pi_{\alpha\beta} = -\eta_{\alpha\beta\gamma\delta}(T)\partial_\gamma u_\delta(\mathbf{r}), \tag{10}$$

where $\eta_{\alpha\beta\gamma\delta}$ is a viscosity tensor. In particular, the momentum current density Π_{xy} in the presence of a transverse velocity gradient $\frac{\partial u_x(y)}{\partial y}$ is given by [25]

$$\Pi_{xy} = -\eta\frac{\partial u_x}{\partial y}, \tag{11}$$

where $\eta \equiv \eta_{xyxy}$ is the coefficient of shear viscosity for an isotropic fluid.

The velocity field $u_x(y)$ gives rise to a perturbation with Hamiltonian

$$H' = -\int d^3r\, u_x(y)\hat{\pi}_x(\mathbf{r}) = \frac{1}{i\omega}\frac{\partial u_x}{\partial y}\int d^3r\, \hat{\Pi}_{xy}. \tag{12}$$

To derive Eq. (12) we have used the conservation law in Eq. (8), integration by parts, and $\hat{\boldsymbol{\pi}}(\mathbf{r},t) = \exp(-i\omega t)\hat{\boldsymbol{\pi}}(\mathbf{r})$. The momentum current density Π_{xy} induced by the perturbation $\hat{H}'$ can be calculated from linear-response theory. The shear viscosity is then obtained by taking the limit $\omega \to 0$:

$$\eta = -\lim_{\omega\to 0}\mathrm{Im}\,\frac{\Xi(\omega)}{\omega} \tag{13}$$

with [24,26]

$$\Xi(\omega) = -i\frac{\hbar}{v}\int d^3r\, dt\, e^{i\omega t}\,\theta(t)\langle[\hat{\Pi}_{xy}(\mathbf{r},t),\hat{\Pi}_{xy}(0,0)]\rangle, \tag{14}$$

where $v = a^3$ is the unit-cell volume and $\theta(t)$ is the Heaviside step function. This formula is the analog of the Kubo expression for the electrical conductivity involving the current-current correlation function.

For a Fermi gas with a quadratic energy dispersion, the momentum current density operator is given by [25]

$$\hat{\Pi}_{xy} = \frac{1}{(2\pi)^3}\int d^3p\,\frac{\hat{p}_x\hat{p}_y}{m}\,\delta f, \tag{15}$$

where $\delta f \equiv f_{\mathbf{k}} - f_{\mathbf{k}}^0$ is the deviation of the distribution function from local equilibrium. For Bloch electrons in a

crystal lattice [27] in a Bloch state $\psi_{\mathbf{k}n}(\mathbf{r}) = \langle \mathbf{r}|n,\mathbf{k}\rangle$, with energy $\epsilon_n(\mathbf{k})$:

$$\frac{\partial \epsilon_n(\mathbf{k})}{\partial k_\alpha} = \frac{\hbar}{im}\int d\mathbf{r}\, \psi^*_{\mathbf{k}n}(\mathbf{r})\frac{\partial \psi_{\mathbf{k}n}(\mathbf{r})}{\partial r_\alpha} = \frac{1}{m}\langle n,\mathbf{k}|\hat{p_\alpha}|n,\mathbf{k}\rangle, \tag{16}$$

where $\epsilon_n(\mathbf{k})$ is the energy dispersion of the nth energy band. Then, (15) can be written

$$\Pi_{xy} = \frac{m}{(2\pi)^3}\int d\mathbf{k}\, v_{k_x} v_{k_y}\delta f \tag{17}$$

with $v_{k_\alpha} = \frac{1}{\hbar}\frac{\partial \epsilon_{\mathbf{k}}}{\partial k_\alpha}$ being the velocity of the Bloch electron. Using *deformation potential* theory [28], a similar result was found by Khan and Allen [29] when investigating sound attenuation by electrons in metals.

It should be pointed out that in a general fluid there are two terms in the stress energy tensor: one associated with the kinetic energy and the second with the interparticle interaction. In dense classical liquids, the terms in the Kubo formula due to the interaction term dominate and are associated with Einstein-Stokes relation where the viscosity is inversely proportional to the particle self-diffusion constant. In contrast, in dilute gases and fluids the kinetic term dominates and the shear viscosity scales with the diffusion constant and scattering time [30]. However, for a zero-range interaction, as in the unitary Fermi gas (and presumably in the Hubbard model), it can be shown that the potential term in the stress tensor does not contribute to the shear viscosity. For a discussion of the above, see around Eq. (7) in Ref. [31].

III. DYNAMICAL MEAN-FIELD THEORY

We consider the single-band Hubbard model with nearest-neighbor hopping, described by the Hamiltonian

$$H = -t\sum_{\langle ij\rangle,\sigma}(c^\dagger_{i\sigma}c_{j\sigma} + \text{H.c.}) - \mu\sum_{i,\sigma} n_{i\sigma} + U\sum_i n_{i\uparrow}n_{i\downarrow}, \tag{18}$$

where $n_{i\sigma} = c^\dagger_{i\sigma}c_{i\sigma}$, t is the hopping amplitude, μ is the chemical potential, and U is the Coulomb repulsion when a given site is doubly occupied by two fermions with opposite spin configuration. Despite its simplicity, this model has no exact solution except in one dimension. The study of this model in higher dimension involves various approximations. However, as in the case of classical mean-field theory for the nearest-neighbor Ising model, in the limit of large dimension $d \to \infty$, the model reduces to an effective single-site model provided we do the scaling $t \to t^*/\sqrt{2d}$ on a d-dimensional hypercubic lattice [32]. Under this approximation we neglect all spatial fluctuations yet fully retain local quantum dynamics. The self-energy $\Sigma_{ij}(\omega)$ for the lattice model then becomes *local*, i.e., $\Sigma_{ij}(\omega) = \Sigma(\omega)\delta_{ij}$. This is known as the dynamical mean-field theory [33] (DMFT) approximation.

It has been found that DMFT gives a good description of the correlation-driven Mott metal-insulator transition observed in $3d$ transition-metal oxides and the crossover from a coherent Fermi liquid to incoherent bad metal state with increasing temperature [5]. Furthermore, DMFT has also been found to provide quantitative description of the resistivity [34] and the frequency-dependent optical conductivity [35] for organic charge-transfer salts that can be described by a half- filled two-dimensional Hubbard model on an anisotropic triangular lattice [36]. DMFT combined with electronic-structure calculations based on density functional theory (DFT) has given an excellent description of a large class of transition-metal and rare-earth compounds [37].

The lattice problem under DMFT can be mapped onto an effective single-impurity Anderson model [33]:

$$H_{\text{imp}} = \sum_{l,\sigma}(\tilde{\epsilon}_l - \mu)c^\dagger_{l\sigma}c_{l\sigma} + \sum_{l,\sigma}(V_l c^\dagger_{l\sigma}d_{0\sigma} + \text{H.c.}) - \mu\sum_\sigma n_{d0\sigma} + U n_{d0\uparrow}n_{d0\downarrow}, \tag{19}$$

where $n_{d0\sigma} = d^\dagger_{0\sigma}d_{0\sigma}$. The operators $d^\dagger_{0\sigma}$ and $d_{0\sigma}$ characterize a local site and $\{c^\dagger_{l\sigma}, c_{l\sigma}\}$ characterizes the effective bath arising from fermions at all other sites. It is important to mention that the fictitious bath dispersion $\tilde{\epsilon}_l$ has no relation to the lattice dispersion $\epsilon_{\mathbf{k}}$.

The solution of the impurity problem is the toughest part and usually involves use of numerical methods such as quantum Monte Carlo (QMC), exact diagonalization (ED), or the numerical renormalization group (NRG). We use iterated perturbation theory (IPT) [38,39] as it is semianalytical, easy to implement, computationally cheap, and fast. Yet, IPT captures the essential physics in the parameter regime $U < 0.8U_c$, where U_c is the critical value of U at which the zero-temperature Mott metal-insulator transition happens. Except in close proximity of the Mott transition, IPT was found to be in good agreement with results from other impurity solvers such as the numerical renormalization group (NRG) [40] and continuous-time quantum Monte Carlo (CTQMC) [41]. In the next subsection, we discuss DMFT self-consistency using IPT.

We briefly mention why it is appropriate to compare the results of AdS/CFT to a calculation involving DMFT. The latter becomes exact in infinite dimension. Generally, AdS/CFT is concerned with finite-dimensional quantum field theories. However, it is found that in certain parameter regimes DMFT can accurately give a quantitative description of quasi-two-dimensional metals near the Mott insulator. Furthermore, connections have been made between the results of AdS/CFT and the infinite-dimensional limit of a model for a gapless spin liquid [42]. We know that the DMFT approximation reduces a lattice problem to an effective local impurity problem which captures local correlation effects. On the other hand, the AdS/CFT correspondence maps a strongly coupled field theory to a problem of fluid mechanics and fluids are characterized by short-range correlations. So, we might expect a DMFT based description of quantum transport of lattice electronic systems will be closely related to quantum transport in the hydrodynamic regime of a strongly coupled field theory.

A. Iterated perturbation theory

The irreducible self-energy in IPT is approximated using the second-order (in U) polarization bubble involving fully interacting bath Green's function $G_0(\omega)$. The self-energy under this approximation can be shown (using moment expansion of the interacting density of states) to smoothly interpolate

between the atomic limit $t = 0$ and the weak-coupling limit $U \to 0$. In the following paragraph we briefly discuss DMFT self-consistency using IPT as the impurity solver. As we are interested in calculating transport properties we work with real frequencies, as against the imaginary frequency formulation that requires analytical continuation of imaginary frequency data to real frequency.

(i) For a given lattice density of states $N_0(\epsilon)$ and self-energy $\Sigma(\omega)$, the *local* Green's function is given by

$$G(\omega) = \int_{-\infty}^{+\infty} \frac{N_0(\epsilon)d\epsilon}{\omega^+ + \mu - \epsilon - \Sigma(\omega^+)}, \tag{20}$$

where μ is the local chemical potential and $\omega^+ = \omega + i\delta$ with $\delta > 0$.

(ii) From the knowledge of the local Green's function $G(\omega)$, we can calculate the *bath hybridization* function $\Delta(\omega)$ by using

$$\Delta(\omega) = \omega^+ + \mu - \Sigma(\omega) - G^{-1}(\omega). \tag{21}$$

(iii) Subsequently using *bath hybridization* we can calculate *bath* Green's function as

$$G_0(\omega) = \frac{1}{\omega + \mu_0 - \Delta(\omega)}. \tag{22}$$

The parameter $\mu_0 = \mu - Un$ is the bath chemical potential and it vanishes at half-filling for the particle-hole symmetric case, which we consider in this study.

(iv) The new self-energy can be calculated using IPT ansatz [39] as

$$\Sigma(\omega) = Un + \frac{A\Sigma^{(2)}(\omega)}{1 - B\Sigma^{(2)}(\omega)}, \tag{23}$$

where

$$A = \frac{n(1-n)}{n_0(1-n_0)}; \qquad B = \frac{U(1-n) - \mu + \mu_0}{n_0(1-n_0)U^2} \tag{24}$$

and n, n_0 are the local and bath particle numbers, respectively. $\Sigma^{(2)}(\omega)$ is the self-energy from second-order perturbation theory and is given by

$$\Sigma^{(2)}(\omega) = U^2 \int_{-\infty}^{+\infty} \prod_{i=1}^{3} [d\epsilon_i \rho_0(\epsilon_i)] \left[\frac{n_F(-\epsilon_1) n_F(\epsilon_2) n_F(-\epsilon_3)}{\omega + i\delta - \epsilon_1 + \epsilon_2 - \epsilon_3} + \frac{n_F(\epsilon_1) n_F(-\epsilon_2) n_F(\epsilon_3)}{\omega + i\delta - \epsilon_1 + \epsilon_2 - \epsilon_3} \right], \tag{25}$$

where $\rho_0(\omega) = -\frac{1}{\pi}\mathrm{Im}[G_0(\omega^+)]$ and $\delta \to 0^+$. We iterate (i)–(iv) until the desired self-consistency in self-energy and other physical quantities are achieved. Here, we consider the particle-hole symmetric case at half-filling $n = 1$. In this case $\mu = \frac{U}{2}$ for all U and T.

B. Shear viscosity in DMFT

Using the self-consistent self-energy, we can calculate the shear viscosity. In the limit of $d \to \infty$, all vertex corrections to two-body correlation functions drop out [43] and the temperature-dependent coefficient of shear viscosity $\eta(T)$, given by the Kubo formula (13), can be calculated using a simple polarization bubble as

$$\eta(T) = \frac{\pi\hbar}{\nu} \int_{-\infty}^{+\infty} d\omega \left[-\frac{\partial n_F(\omega)}{\partial \omega} \right] \int_{-\infty}^{+\infty} d\epsilon\, \Theta_{xy}(\epsilon) A^2(\omega, \epsilon), \tag{26}$$

where $\nu = a^d$ is the volume of the unit cell of a d-dimensional hypercubic lattice with lattice constant a,

$$A(\omega, \epsilon) = -\frac{1}{\pi}\mathrm{Im}\left[\frac{1}{\omega^+ + \mu - \epsilon - \Sigma(\omega^+)} \right], \tag{27}$$

$$n_F(\omega) = \frac{1}{e^{\beta\omega} + 1} \tag{28}$$

are the spectral density and Fermi function, respectively,

$$\Theta_{xy}(\epsilon) = \frac{m^2}{N} \sum_{\mathbf{k}} v_{kx}^2 v_{ky}^2 \delta(\epsilon - \epsilon_{\mathbf{k}}) \tag{29}$$

with $v_{k\alpha} = \frac{1}{\hbar}\frac{\partial \epsilon_{\mathbf{k}}}{\partial k_\alpha}$ is the *transport density of states for the shear viscosity*, and N is the number of lattice sites. Following a similar procedure to that in Ref. [44], we can show that the transport density of states for shear viscosity for a d-dimensional hypercubic lattice with nearest-neighbor hopping is given by

$$\Theta_{xy}(\epsilon) = \frac{\gamma^2}{2d(d-1)} \left[-\frac{3}{2} M_3(\epsilon) + 2\epsilon M_2(\epsilon) + \left(4dt^2 - \frac{1}{2}\epsilon^2 \right) M_1(\epsilon) - 4t^2 \epsilon M_0(\epsilon) \right], \tag{30}$$

where $\gamma = \frac{ma^2}{\hbar^2}$ and

$$M_n(\epsilon) \equiv \int_{-\infty}^{\epsilon} z^n N_0(z) dz, \tag{31}$$

where $N_0(\epsilon) = \sum_{\mathbf{k}} \delta(\epsilon - \epsilon_{\mathbf{k}})$ is the *density of states* per spin. In the Appendix, we give a detailed derivation of this important result. In the following subsections, we explicitly evaluate this expression for the hypercubic lattice and Bethe lattice cases.

One should consider how the vertex corrections could modify the DMFT results in finite dimensions. For the unitary Fermi gas vertex corrections increase the viscosity by a factor of about 2.6 [compare the discussion below Eq. (54) in Ref. [31]]. For the quark-gluon plasmon in the theory of quantum chromodynamics (QCD) at high temperatures vertex corrections significantly increase the viscosity, changing the functional dependence on the coupling constant [compare Eqs. (4.25) and (4.26) in Ref. [45]]. In a two-dimensional Fermi liquid, the vertex corrections have been shown [46] to be of the order of $[\ln(E_F/T)]^3$. For a doped Hubbard model, it was found in a dynamical cluster approximation calculation based on a four-site cluster that the vertex corrections to the optical conductivity were not significant, except very close to the Mott insulator [47]. A study of the same model using a two-particle self-consistent approach found that vertex corrections changed the calculated resistivity by less than a factor of 2 [48]. In light of the above, it seems unlikely that vertex corrections would increase the viscosity by more than an order of magnitude compared to the DMFT results.

1. Hypercubic lattice case

For hypercubic lattice in the limit of $d \to \infty$, we have $N_0(\epsilon) = \frac{1}{\sqrt{\pi}t^*} \exp[-\epsilon^2/t^{*2}]$ for the density of states. It is important to mention that the chosen density of states in the limit $d \to \infty$ requires the scaling $2t \to t^*/\sqrt{d}$. The transport density of states for the shear viscosity is then given by

$$\Theta_{xy}(\epsilon) = \frac{\gamma^2 t^{*3}}{2d(d-1)}[-3I_3(\tilde{\epsilon}) + 4\tilde{\epsilon} I_2(\tilde{\epsilon}) - \tilde{\epsilon}^2 I_1(\tilde{\epsilon}) + 2I_1(\tilde{\epsilon}) - 2\tilde{\epsilon} I_0(\tilde{\epsilon})], \quad (32)$$

where

$$I_n(x) = \frac{1}{\sqrt{\pi}} \int_{-\infty}^{x} u^n e^{-u^2} du \quad (33)$$

are the dimensionless integrals and $\tilde{\epsilon} = \epsilon/t^*$ is the dimensionless energy.

We define the scaled dimensionless transport density of states for the shear viscosity $\bar{\Theta}(\tilde{\epsilon})$ as

$$\bar{\Theta}_{xy}(\tilde{\epsilon}) = -3I_3(\tilde{\epsilon}) + 4\tilde{\epsilon} I_2(\tilde{\epsilon}) - (\tilde{\epsilon}^2 - 2)I_1(\tilde{\epsilon}) - 2\tilde{\epsilon} I_0(\tilde{\epsilon}). \quad (34)$$

Using the exact integrals

$$\int_{-\infty}^{\epsilon} \left(z^2 - \frac{1}{2}\right) e^{-z^2} dz = -\frac{1}{2}\epsilon e^{-\epsilon^2}, \quad (35)$$

$$\int_{-\infty}^{\epsilon} z e^{-z^2} dz = -\frac{1}{2} e^{-\epsilon^2}, \quad (36)$$

$$\int_{-\infty}^{\epsilon} z^3 e^{-z^2} dz = -\frac{1}{2}(\epsilon^2 + 1) e^{-\epsilon^2}, \quad (37)$$

we get

$$\bar{\Theta}_{xy}(\tilde{\epsilon}) = \frac{1}{2} N_0(\tilde{\epsilon}) = \frac{1}{2\sqrt{\pi}} e^{-\tilde{\epsilon}^2}. \quad (38)$$

In Fig. 1(a), we show transport density of states for viscosity for hypercubic lattice. Interestingly, the transport density of states for electrical conductivity for hypercubic lattice also follows a relation similar to Eq. (38), as shown in Ref. [44].

The shear viscosity is then given by

$$\eta = \eta_0^b \int_{-\infty}^{+\infty} d\tilde{\omega} \left[-\frac{\partial n_F(\tilde{\omega})}{\partial \tilde{\omega}}\right] \int_{-\infty}^{+\infty} d\tilde{\epsilon}\ \bar{\Theta}_{xy}(\tilde{\epsilon}) A^2(\tilde{\omega}, \tilde{\epsilon}), \quad (39)$$

where the dimensionful prefactor η_0^b is given by Eq. (6) with $m_b = \frac{\hbar^2}{a^2 t^*}$ and $\tilde{\omega} = \omega/t^*$ is the dimensionless energy.

2. Bethe lattice case

We consider the Bethe lattice (Cayley tree) with coordination number z. In the limit of infinite coordination number ($z \to \infty$), the density of states has *semicircular* form [49]

$$N_0(\epsilon) = \frac{2}{\pi W^2} \sqrt{W^2 - \epsilon^2}\ \theta(W - |\epsilon|), \quad (40)$$

where $\theta(x)$ is the Heaviside step function, $W = 2t^*$ is the half-bandwidth, and the nearest-neighbor hopping amplitude (t) in this case is scaled as $t \to t^*/\sqrt{z}$. For a Bethe lattice with coordination number z, the connectivity $K = z - 1$ while that for a d-dimensional hypercubic lattice is $2d$. So, in the limit of large coordination number we can always do the mapping $z \leftrightarrow 2d$. Because of its treelike structure, the Bethe lattice has no closed loop and hence no energy dispersion with Bloch wave vector $\mathbf{k}$. However, by invoking the f-sum rule we can still calculate $\Theta_{xy}(\epsilon)$. For the given density of states we then have the following exact integrals [44]:

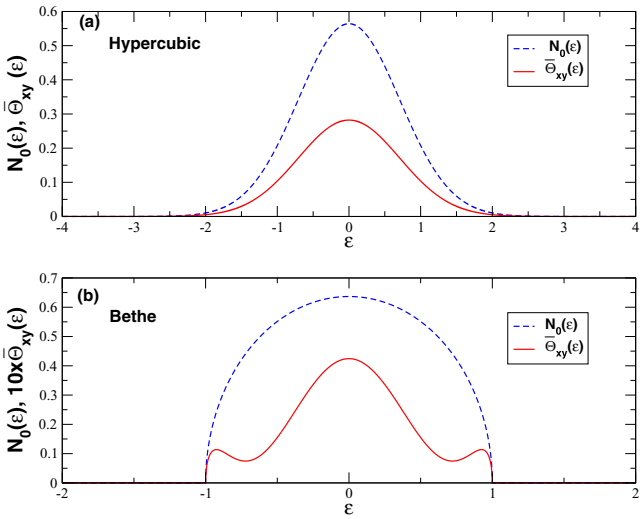

FIG. 1. (Color online) Density of states $N_0(\epsilon)$ and scaled dimensionless transport density of states for shear viscosity $\bar{\Theta}_{xy}(\epsilon)$ for the hypercubic lattice [panel (a)] and for the Bethe lattice [panel (b)]. $\bar{\Theta}_{xy}(\epsilon)$ for the Bethe lattice shows additional structures near the band edges, but for the hypercubic lattice it is just proportional to the density of states. $\bar{\Theta}_{xy}(\epsilon)$ for the Bethe lattice has been multiplied by a factor of 10 to show both curves in the same panels. Energies have been scaled by the effective hopping amplitude t^* in the case of the hypercubic lattice and by the half-bandwidth W in the case of the Bethe lattice.

$$M_0(\epsilon) = \frac{1}{2}\epsilon N_0(\epsilon) + \frac{1}{2} + \frac{1}{\pi} \tan^{-1}\left[\frac{\epsilon}{\sqrt{W^2 - \epsilon^2}}\right], \quad (41)$$

$$M_1(\epsilon) = -\frac{1}{3}(W^2 - \epsilon^2) N_0(\epsilon), \quad (42)$$

$$M_2(\epsilon) = -\frac{\epsilon(W^2 - 2\epsilon^2)}{8} N_0(\epsilon) + \frac{W^2}{8} + \frac{W^2}{4\pi} \tan^{-1}\left[\frac{\epsilon}{\sqrt{W^2 - \epsilon^2}}\right], \quad (43)$$

$$M_3(\epsilon) = \frac{1}{120} N_0(\epsilon)[18\epsilon^4 - 5\epsilon^2 W^2 - 16W^4]. \quad (44)$$

Then, by replacing these exact analytical integrals into the expression in Eq. (30) for $\Theta_{xy}(\epsilon)$ and using $W = 2t\sqrt{2d}$ we get

$$\Theta_{xy}(\epsilon) = \frac{\gamma^2}{240d(d-1)} N_0(\epsilon)[8W^4 - 25\epsilon^2 W^2 + 26\epsilon^4]. \quad (45)$$

It is interesting to mention that the constant term as well as the $\tan^{-1}[\frac{\epsilon}{\sqrt{W^2-\epsilon^2}}]$ term cancels out in the final expression for $\Theta_{xy}(\epsilon)$.

In Fig. 1(b), we show the scaled dimensionless transport density of states $\bar{\Theta}_{xy}(\tilde{\epsilon})$:

$$\bar{\Theta}_{xy}(\tilde{\epsilon}) = \tfrac{1}{120} N_0(\tilde{\epsilon})(8 - 25\tilde{\epsilon}^2 + 26\tilde{\epsilon}^4) \tag{46}$$

with $\tilde{\epsilon} = \epsilon/W$ for the Bethe lattice. Near the band edges ($\tilde{\epsilon} = \pm 1$) $\bar{\Theta}_{xy}(\tilde{\epsilon})$ shows nonmonotonic structures in contrast to the density of states $N_0(\tilde{\epsilon}) = \frac{2}{\pi}\sqrt{1-\tilde{\epsilon}^2}$, which is always monotonic near the band edges.

The expression in Eq. (26) for the shear viscosity for the Bethe lattice is then given by Eq. (39) where the dimensionful prefactor η_0^b is given by Eq. (6) with $m_b = \frac{\hbar^2}{a^2 W}$ and $\tilde{\omega} = \omega/W$ is the dimensionless energy.

C. Entropy density

The total internal energy in DMFT is given by [50]

$$\frac{E(T)}{N} = k_B T \sum_{n,\sigma} \int_{-\infty}^{+\infty} d\epsilon \frac{\epsilon N_0(\epsilon)}{i\omega_n + \mu - \Sigma_\sigma(i\omega_n) - \epsilon} + \frac{1}{2}\sum_{n,\sigma} \Sigma_\sigma(i\omega_n) G_\sigma(i\omega_n), \tag{47}$$

where N is the total number of particles in the system, $\omega_n = (2n+1)\pi k_B T$ is the Matsubara frequency, and $N_0(\epsilon)$ is the noninteracting density of states. In the paramagnetic state, Eq. (47) can be expressed as a real frequency integral

$$\frac{E(T)}{N} = 2\int_{-\infty}^{+\infty} d\omega\, n_F(\omega)(\omega+\mu)A(\omega) + \frac{1}{\pi}\int_{-\infty}^{+\infty} d\omega\, n_F(\omega)\mathrm{Im}[\Sigma(\omega^+)G(\omega^+)], \tag{48}$$

where $A(\omega) = -\frac{1}{\pi}\mathrm{Im}[G(\omega^+)]$ is the spectral function.

From $E(T)$ we can calculate the specific heat using $C_v(T) = (\frac{\partial E(T)}{\partial T})_v$ and then we can calculate the local entropy density $s(T)$ as

$$s(T) = \frac{1}{v}\int_0^T \frac{C_v(T')}{T'} dT', \tag{49}$$

where v is the volume of the system. The temperature dependence of the specific heat and the entropy for the half-filled Hubbard model have both been calculated previously using a range of impurity solvers including IPT and quantum Monte Carlo [50–52]. It is found that in the metallic phase, the entropy density is linear in temperature below the Fermi liquid coherence temperature T_{coh} and becomes of order $nk_B \ln(2)$ for $T \sim T_{\mathrm{coh}}$, where n is number density of fermions.

D. Quantum limits

The quantum limit of the shear viscosity $\eta_q = \frac{1}{5} n\hbar$ is based on the free-particle dispersion $E_{\mathbf{k}} = \frac{\hbar^2 k^2}{2m}$ in the continuum limit. For a discrete lattice model, we need to derive an appropriate quantum limit for shear viscosity.

For temperatures and frequencies much less than the coherence scale (i.e., $T \ll T_{\mathrm{coh}}$, $\omega \ll k_B T_{\mathrm{coh}}$ where T_{coh} is the coherence temperature which is of the order of the Kondo temperature for the corresponding single-impurity Anderson model), the self-energy $\Sigma(\omega)$ has the Fermi liquid form

$$\Sigma(\omega, T) = \omega\left(1 - \frac{1}{Z}\right) - iC[\omega^2 + (\pi k_B T)^2], \tag{50}$$

where Z is the quasiparticle renormalization factor and C is a positive constant.

Following the procedure in Ref. [5] used to estimate the Mott-Ioffe-Regel limit for the conductivity we can show that at low temperature ($T \ll T_{\mathrm{coh}}$), the shear viscosity for the hypercubic lattice is given by

$$\eta(T) = \eta_0^b \bar{\Theta}_{xy}(0) I_{01} \pi^2 t^* \tau(T)/\hbar, \tag{51}$$

where $I_{01} \simeq 0.08$ is a dimensionless integral and $\hbar/\tau(T) = -\mathrm{Im}[\Sigma(\omega = 0, T)]$ is the quasiparticle decay rate. The quantum limit to shear viscosity will then correspond to $t^* \sim \hbar/\tau(T)$ and we will have the quantum limit to shear viscosity

$$\eta_q^{\mathrm{lat}} = \frac{1}{2\sqrt{\pi}}\eta_0^b \tag{52}$$

for the hypercubic lattice and

$$\eta_q^{\mathrm{lat}} = \frac{2}{15\pi}\eta_0^b \tag{53}$$

for the Bethe lattice.

IV. PARAMETERS FOR LIQUID ^{3}He

We consider liquid ^{3}He because of the availability of extensive experimental data for the temperature and pressure dependence of the shear viscosity, recently reviewed and parametrized by Huang *et al.* [2]. First, we review how liquid ^{3}He might be described as a lattice gas with a Hubbard model Hamiltonian.

Low-temperature properties of liquid ^{3}He can be described by Landau's Fermi liquid theory. The effective mass of the quasiparticles (as deduced from the specific heat) is about three times the bare mass m at 0 bar pressure and increases to six times at 33 bar, when the liquid becomes solid. The compressibility is also renormalized and decreases significantly with increasing pressure. This led Anderson and Brinkman to propose that ^{3}He was an "almost localized" Fermi liquid. Thirty years ago, Vollhardt worked this idea out in detail, considering how these properties might be described by a lattice gas model with a Hubbard Hamiltonian [53]. The system is at half-filling with U increasing with pressure, and the solidification transition (complete localization of the fermions) then has some connection to the Mott transition. All of the calculations of Vollhardt were at the level of the Gutzwiller approximation (equivalent to Kotliar-Ruckenstein slave-boson mean-field theory). A significant result from the theory is that it describes the weak pressure dependence and value of the Sommerfeld-Wilson ratio of the spin susceptibility to the specific heat (which is related to the Fermi liquid parameter F_0^a). At ambient pressure U was estimated to about 80% of the critical value U_c for the Mott transition. Vollhardt, Wolfle, and Anderson [54] also considered a more realistic situation where the system is not at half-filling. Then, the doping (band filling) is determined by the ratio of the molar volume of the liquid to the molar volume of the solid (which by definition corresponds to half-filling). Finite-temperature

extension to Volhardt theory was done by Seiler, Gros, Rice, Ueda, and Vollhardt [55]. Later, Georges and Laloux [56] argued ^{3}He is a Mott-Stoner liquid, i.e., one also needs to take into account the exchange interaction and proximity to a Stoner ferromagnetic instability. If this Mott-Hubbard picture is valid for ^{3}He, then one should also see a crossover from a Fermi liquid to a "bad metal" with increasing temperature. Specifically, above some "coherence" temperature $T_{\rm coh}$, the quasiparticle picture breaks down. For example, the specific heat per atom should increase linearly with temperature up to a value of order k_B around $T_{\rm coh}$, and then decrease with increasing temperature. Indeed, one does see this crossover in experimental data (compare Fig. 1 in Ref. [57]).

We now consider what Hubbard model parameters are appropriate for ^{3}He. The density at a pressure of 1 bar, $n \simeq N_A/(37\ {\rm cm}^3)$ (where $N_A = 6.023 \times 10^{23}$ is the Avogadro number) increases monotonically to $n \simeq N_A/(26\ {\rm cm}^3)$ at 33 bar (near the solidification pressure) (see Table III in Ref. [58]).

The band mass m_b can be written in terms of $E_F = \hbar^2 k_F^2/(2m)$, the noninteracting Fermi energy, and the band energy E_b as

$$\frac{m}{m_b} = \frac{1}{2}(ak_F)^2 \frac{E_b}{E_F} = \frac{1}{2}(3\pi^2)^{2/3}\frac{E_b}{E_F} \simeq 4.8\frac{E_b}{E_F}, \qquad (54)$$

where we have used the fact that $n = 1/a^3 = k_F^3/(3\pi^2)$.

There are several ways to estimate the band energy scale. If we have a Bethe lattice, then $E_b = W = E_F$, at half-filling. Alternatively, we can compare the noninteracting density of states per spin at the Fermi energy $N_0(0)$. This has the value of $3/(4E_F)$, $2/(\pi W)$, and $1/(\sqrt{\pi}t^*)$ for the cases of a parabolic band (free fermions), Bethe lattice, and hypercubic lattice, respectively. Setting these equal gives $E_b \equiv W = 8E_F/(3\pi) \simeq 0.85E_F$ and $E_b \equiv t^* = 4E_F/(3\sqrt{\pi}) \simeq 0.75E_F$. Using the density at 1 bar and the noninteracting expression $E_F = \hbar^2 k_F^2/(2m)$, we estimate $T_F \simeq 4.95$ K, and so $t^* \simeq 3.72$ K.

In the following sections, we compare some of our calculations of the shear viscosity with experimental data for ^{3}He. Huang *et al.* [2] showed that the shear viscosity of saturated liquid ^{3}He from 3 mK to 0.1 K follows the Fermi liquid relation $\eta \propto 1/T^2$. Furthermore, they showed that the shear viscosity data in the range from 3 mK to near the critical point at 3.31 K, collected over the past 50 years from various experimental groups, can be fitted to the empirical form

$$\eta(T) = \frac{c_1}{T^2} + \frac{c_2}{T^{1.5}} + \frac{c_3}{T} + c_4 \qquad (55)$$

with $c_1 = 2.897\times10^{-7}$ Pa·s K^2, $c_2 = -7.02\times10^{-7}$Pa · s K$^{1.5}$, $c_3 = 2.012 \times 10^{-6}$ Pa · s K, and $c_4 = 1.323 \times 10^{-6}$ Pa · s. We note that at low temperatures, Eq. (55) has a Fermi liquid term. At high temperatures, Eq. (55) has the asymptotic value of c_4 which is comparable to $n\hbar \simeq 1.6 \times 10^{-6}$ Pa · s at 1 bar pressure. It should be pointed out that this is for data along the liquid-vapor curve and so the pressure gradually increases with temperature. However, as the critical pressure is about 100 kPa, much less than the melting pressure, this pressure dependence is not significant. The viscosity decreases by a factor of at most 10 as the pressure increases from 1 kPa to 3 MPa (the melting pressure) for all temperatures below 1 K. Huang *et al.* fitted all the available experimental data to an expansion in terms of Chebyshev polynomials and used this to plot the temperature dependence for pressures ranging from 1 kPa to 20 MPa (compare Fig. 8 in Ref. [2]). For pressures larger than about 500 kPa, the viscosity has a nonmonotonic temperature dependence with a minimum around a temperature of 1 K.

V. RESULTS

We consider the case of half-filling, $n = 1$, i.e., each site on the average is occupied by one fermion. We study the shear viscosity and the entropy density as a function of correlation strength U and temperature T.

In Figs. 2(a) and 2(b), we show the scaled shear viscosity $\eta(T)/\eta_0^b$ as a function of temperature for various interaction strengths U, for the hypercubic and the Bethe lattice, respectively. Similar results are obtained for both lattices.

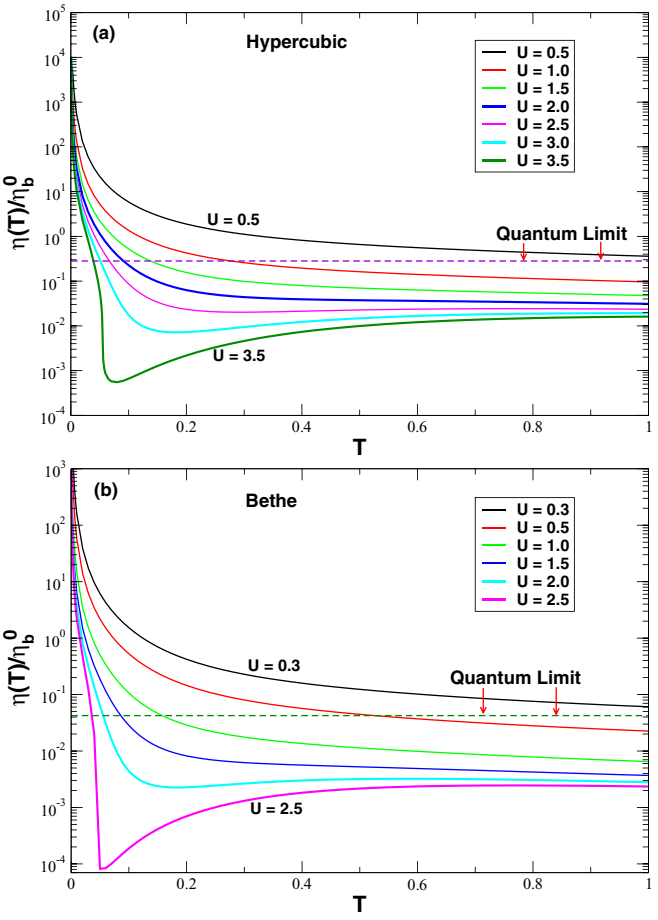

FIG. 2. (Color online) Shear viscosity $\eta(T)/\eta_0^b$ as a function of temperature for a range of interaction strengths U. Results are shown for both the hypercubic lattice [panel (a)] and the Bethe lattice [panel (b)]. Solid lines correspond to DMFT based numerical results. T and U are measured in units of W for the Bethe lattice and in units of t^* for the hypercubic lattice case. Note that as the Mott insulator is approached, the shear viscosity becomes extremely small. The dashed lines are the quantum limits given by Eqs. (52) (hypercubic lattice) and (53) (Bethe lattice).

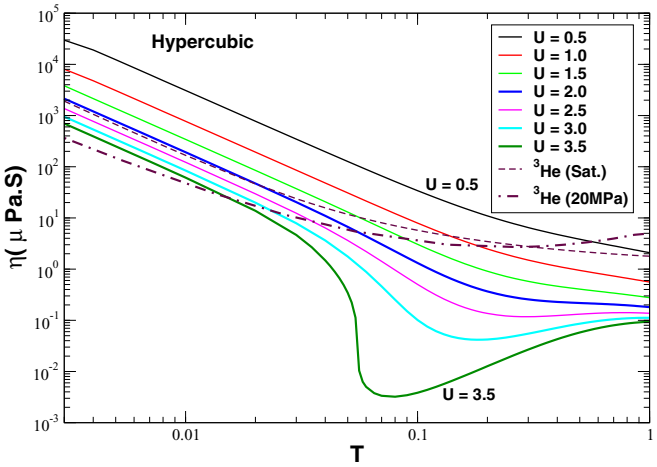

FIG. 3. (Color online) Shear viscosity $\eta(T)$ on a log-log plot clearly shows $1/T^2$ behavior in the low-temperature region, characteristic of a Fermi liquid. At high temperatures, there is significant deviation from the Fermi liquid behavior as the Mott transition is approached. The upper dashed line corresponds to experimental data for saturated liquid ^{3}He parametrized by Eq. (55). The lower dashed line is at a higher pressure. The results are shown for the hypercubic lattice case with the parameters $t^* = 3.72$ K and $m_b/m = 3.6$. Both T and U are measured in units of t^*.

A. Quantum limits

We consider violation of quantum limit of shear viscosity. In the weakly correlated hypercubic lattice system with $U = 0.5$, the shear viscosity is always above quantum limit $\eta_q^{\rm lat} \simeq 0.28\eta_0^b$, but as we increase the interaction strength U, the shear viscosity smoothly goes below the quantum limit with increasing temperature T. This corresponds to the fact that at low temperatures ($T \ll T_{\rm coh}$), the quantum transport is due to coherent quasiparticle states but at high temperatures ($T > T_{\rm coh}$) the transport becomes incoherent in nature. This is the analog of how in bad metals the resistivity smoothly increases above the Mott-Ioffe-Regel limit.

B. Low-temperature behavior

Figure 3 clearly shows that the shear viscosity follows Fermi liquid characteristic $1/T^2$ behavior in the low-temperature region ($T \ll T_{\rm coh}$). The range of Fermi liquid behavior decreases with increasing U. This is because the coherence scale (and Kondo temperature for the corresponding single-impurity Anderson model) decreases with increasing correlation strength U. The $1/T^2$ behavior is similar to the low-temperature behavior of the electrical conductivity and the quantum transport in this region can be characterized by coherent quasiparticle states.

Our calculated shear viscosity shows qualitative behavior consistent with experimental data for liquid ^{3}He, using parameters estimated in the previous section. There is qualitative as well as quantitative agreement at low temperatures but not at higher temperatures. Interestingly, our calculated shear viscosity for $U = 2$ for the hypercubic lattice nearly fits with the experimental results at low temperatures. Our calculation suggests ^{3}He is a moderately correlated system with $U/U_c \sim 0.5$ ($U_c \sim 4.0$ for the hypercubic lattice) as against the suggestion of Volhardt [53] that ^{3}He is a nearly localized Fermi liquid with $U/U_c \sim 0.8$ at 1 bar pressure and $U/U_c \sim 0.9$ close to the melting pressure. It is important to mention that Gutzwiller based static mean-field theory overestimates local correlation effects but the self-consistent treatment of dynamic correlation effects in DMFT renormalizes local correlation effects.

C. High-temperature behavior

In the high-temperature region $T \gg T_{\rm coh}$, the shear viscosity shows significant deviation from the low-temperature Fermi liquid behavior as can be observed from Figs. 2 and 3. The quantum transport in this region is incoherent in nature. For the weakly and moderately correlated systems, the deviation is smooth and monotonic but for strongly correlated systems for $U = 2.5$ and above the deviation is much sharper and nonmonotonic. This is due to the sharp crossover between the Fermi liquid fixed point and the local moment fixed point in the strongly correlated regime. A similar nonmonotonic temperature dependence is seen in the electrical resistivity from DMFT calculations and in organic charge-transfer salts close to the Mott insulator [5,23,34].

D. Entropy density

In Fig. 4, we show the entropy density $s(T)$ as a function of temperature for various interaction strengths. At high temperatures, the entropy density approaches ln(4) which arises due to local charge and spin fluctuations. As the temperature decreases, charge fluctuations freeze-out and the model can be described by localized weakly interacting spin $\frac{1}{2}$'s with characteristic entropy density ln(2). Finally, in the Fermi liquid state the local spin degrees of freedom are

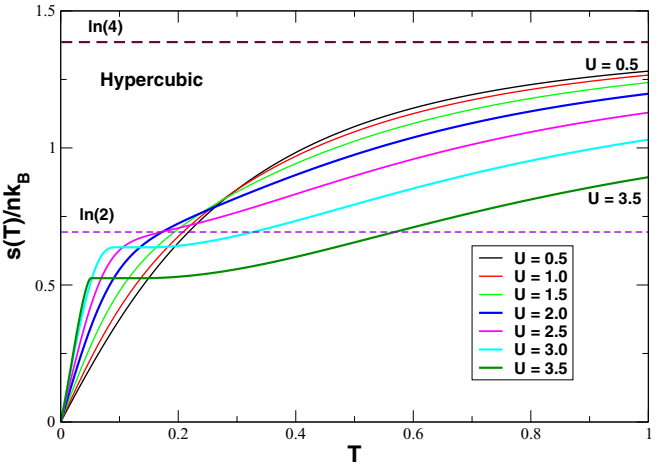

FIG. 4. (Color online) Entropy density $s(T)$ (in units of nk_B) as a function of temperature T for various interaction strength U. Below the coherence temperature $T_{\rm coh}$, the entropy is linear in temperature, characteristic of a Fermi liquid. The crucial point is that for $T > T_{\rm coh}$, the entropy is of order nk_B. The kinklike feature for $U = 2.5$ and above corresponds to the formation of poorly screened local moment and its position is closely related to $T_{\rm coh}$. The calculation is for the hypercubic lattice and both T and U are measured in units of t^*.

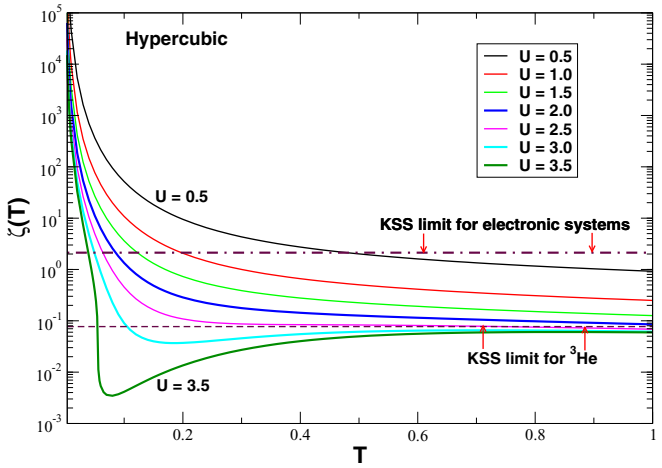

FIG. 5. (Color online) Dimensionless scaled ratio $\zeta(T)$ of the shear viscosity and entropy density. [See Eq. (56) for definition of $\zeta(T)$.] It is shown as a function of temperature T for various interaction strength U. Dashed and dotted-dashed lines correspond to the Kovtun-Son-Starinets (KSS) limit for ^{3}He and typical lattice electronic systems, respectively. For electronic systems, there is strong violation of the quantum bound for $T \gg T_{\rm coh}$. The calculation is for the hypercubic lattice case and both T and U are measured in units of t^*.

dynamically screened and the entropy density vanishes linearly in temperature. For weakly and moderately correlated electron system, the entropy density smoothly crosses over ln(2). But, for strongly correlated electron systems with $U = 2.5$ and above, a kinklike feature develops. This corresponds to formation of poorly screened local moment. The position of the kink in the specific heat versus temperature curve is related to the coherence temperature $T_{\rm coh}$ [59]. For extremely correlated systems with $U = 3.0$ and above, the entropy density given by iterated perturbation theory (IPT) is underestimated. Consequently, the specific heat in the coherent-incoherent crossover region becomes negative, which is unphysical. This is due to an incorrect total energy estimate in IPT which has been reported in earlier literature (see, for example, Fig. 7 in Ref. [52]) [60]. In the unphysical temperature range we set the specific heat to zero and the calculated entropy density, which is an integrated quantity, will deviate by not more than 5% from the actual value. Such a small error has little effect on whether the Kovtun-Son-Starinets (KSS) bound is violated.

E. Possible violation of the KSS bound

Finally, we consider the dimensionless scaled shear viscosity $\eta(T)$, entropy density $s(T)$, ratio

$$\zeta(T) \equiv \frac{\eta(T)}{s(T)} \frac{4\pi k_B}{\hbar} \left(\frac{m_b}{m}\right)^2. \tag{56}$$

At the KSS bound $\zeta(T) = (\frac{m_b}{m})^2$ (for $d = 3$). As stressed before, this depends on the material properties t^* and a as well as the mass of the fermion m.

In Fig. 5, we show $\zeta(T)$ and compare to its value against the Kovtun-Son-Starinet (KSS) limit for parameters appropriate for ^{3}He and typical lattice electronic systems such as cuprates and organic superconductors.

For cuprates [61], the hopping integral $t \simeq 0.18$ eV, $a = 3.9$ Å and for organic charge-transfer salts [36] $t \simeq 0.05$ eV, $a = 8$ Å. For these systems $d = 2$ and hence $t^* = 2t\sqrt{d} \equiv 2\sqrt{2}t$. This will give $m/m_b \simeq 1.0$ for cuprates and $m/m_b \simeq 1.2$ for organics, as compared to $m/m_b \simeq 3.6$ for liquid ^{3}He. As a result, the shear viscosity for these lattice electronic systems will be smaller by a factor of about 10 than for the charge-neutral fermionic fluid ^{3}He. Straub and Harrison considered a simple model for the hopping integral for d bands in transition metal [62]. This gives for d-sigma bands $m/m_b \simeq 2.8(r_d/a)^3$, where r_d is approximately the d-state radius and of the order of the radius transition metal atom, $\sim$1 Å. In principle then for a system with a large lattice constant, the bandwidth can be very small and values of m/m_b even smaller than unity are possible. In an ultracold fermionic atom system in an optical lattice one could in principle then make m/m_b, and thus the viscosity, extremely small.

From Fig. 5, we can clearly see that for all $U < 3.0$ and for ^{3}He parameters $\zeta(T)$ is above the KSS limit. For extremely correlated system $U = 3.5$, there is strong violation of the limit in the crossover region, but even for this system at high temperature the bound seems to be respected [within numerical error in calculation of entropy density $s(T)$]. Also, in the high-temperature region, the scaled ratio seems to approach some universal limit.

For electronic lattice systems, the limit is well respected in the coherent quasiparticle regime of transport but the limit is violated in the region $T > T_{\rm coh}$. This is due to reduction of the shear viscosity by a factor of 10 compared to ^{3}He parameters. The violation is as large as 1000% for these systems, when they are close to the Mott transition.

VI. EXPERIMENTAL DETERMINATION OF η IN ELECTRONIC SYSTEMS

Given our result that the KSS bound can be violated in a bad metal, it is highly desirable that experimental measurements be performed on candidate strongly correlated electron materials such as organic charge-transfer salts and cuprates. Unfortunately, at present there is no direct measurement of the shear viscosity for electronic systems. Recently, an indirect estimate of η/s was made from angle-resolved photoemission spectroscopy (ARPES) experiments in cuprates [63] giving a value comparable to the KSS limit. However, it should be stressed that neither the viscosity nor the entropy were directly measured. Rather, the ARPES line shape was used to estimate the quasiparticle lifetime and the state occupation. The viscosity was then estimated from the lifetime. The entropy was estimated from an expression in terms of the state occupations in a noninteracting fermion system. In the incoherent regime of transport, this method will not be applicable. It is important to mention that our calculation showed that in the coherent quasiparticle regime of transport, η/s is always above the KSS bound and hence our result is consistent with these experimental results.

A more direct way to measure the viscosity of the electron fluid in a metallic crystal is through the attenuation of sound, as first emphasized by Mason [64]. A more sophisticated and

general theory was developed by Kahn and Allen [29]. The connection between shear viscosity and ultrasound attenuation can be loosely motivated by Stokes law, given in Eq. (2). In a metal, provided the wavelength of sound is much larger than the electronic mean-free path, then one is in the hydrodynamic limit, and the attenuation is given by a similar expression to Stokes law (with appropriate indices for crystal axes), with ρ the solid density, not that of the electron fluid. In a simple free-electron model, Eq. (3) shows that the electronic viscosity is proportional to the scattering time, just like the electrical conductivity. Hence, the ultrasound attenuation should scale with the conductivity. Indirect evidence for this idea was found from the temperature dependence of ultrasound attenuation in aluminium [65], including the predicted quadratic frequency dependence. In clean metals, the attenuation (and viscosity) becomes very large at low temperatures, making it easier to measure. Also, for high-frequency ultrasound, one can reach the "quantum regime" where the mean-free path becomes comparable to the sound wavelength. Pippard worked out a general theory describing the crossover from the hydrodynamic regime to this quantum regime [66]. In bad metals, could one experimentally measure the small electronic viscosity of the order of $n\hbar$? First, the small mean-free path, characteristic of bad metals, means one will always be in the hydrodynamic regime. However, the small viscosity means that the sound attenuation due to the electron fluid will be small and possibly dominated by other sources of attenuation such as crystal dislocations. A rough estimate for an electron viscosity of order of $n\hbar$ and a sound frequency of 1 GHz give an attenuation of less than 0.1 cm^{-1}, of the order of typical sensitivity, such as in measurements for heavy-fermion compounds [67].

Resonant ultrasound spectroscopy (RUS) [68–70] has been used to make measurements on strongly correlated electron systems [71–73]. The spectrum is determined by the resonant elastic modes of the sample; they are determined by the sample shape and orientation, elastic constants, and dissipation. RUS allows determination of the elastic constant tensor C_{ij} from measurements on small samples (<1 mm^3 volume). In the regime where the attenuation of the ultrasound is dominated by coupling to the electrons, rather than fluctuations associated with phase transitions, the viscosity could be determined from the damping (frequency width $\Delta\omega$) of the resonances. We estimate $\Delta\omega/\omega \sim \eta\omega/C_{ij}$ [1] and so for the MHz frequencies typically used in RUS, the damping associated with a viscosity of order $n\hbar$ requires an oscillator Q factor of order 10^{10} and so is unlikely to be observable.

Recently, several new approaches have been suggested to experimentally measure the viscosity of the electron fluid in a metallic crystal. Forcella, Zaanen, Valentinis, and van Der Marel [74] considered electromagnetic properties of viscous charged fluids, finding signatures due to the viscosity such as negative refraction, a frequency-dependent peak in the reflection coefficient, and a strong frequency dependence of the phase. However, they note that these effects may be difficult to observe for viscosities of the order of $n\hbar$. Tomadin, Vignale, and Polini [75] considered a two-dimensional electron fluid in a Corbino disk device in the presence of an oscillating magnetic flux. They showed that the viscosity could be determined from the dc potential difference that arises between the inner and the outer edges of the disk. In particular, for viscosities of the order of $n\hbar$ the potential difference varied significantly oscillation frequencies in the MHz range. Levitov and Falkovich [76] recently considered the flow of an electron fluid in a micrometer scale channel in the hydrodynamic regime, where the electron-electron collision rate is much larger than the momentum relaxation rate. They found that when the viscosity to resistance ratio is sufficiently large, viscous flow occurs producing vorticity and a negative nonlocal voltage. Spatially resolved measurements of the voltage allow determination of the viscosity. Torre, Tomadin, Geim, and Polini [77] considered the electron liquid in graphene in the hydrodynamic regime and showed that the shear viscosity could be determined from measurements of nonlocal resistances in multiterminal Hall bar devices. Although these proposals are promising for the two-dimensional electron fluids in graphene and semiconductor heterostructures fabrication of the relevant micron-scale devices may be particularly challenging for bad metals such as cuprates and organic charge-transfer salts.

VII. CONCLUSIONS

We have studied the shear viscosity, the entropy density, and their ratio for a single-band Hubbard model using single-site dynamical mean-field theory. Similar results were obtained for the density of states associated with both hypercubic and Bethe lattices. We compared our results for the temperature dependence of the shear viscosity to experimental results for liquid ^{3}He. The calculated shear viscosity shows qualitative as well as quantitative behavior consistent with experimental results. At low temperatures, the shear viscosity is proportional to $1/T^2$ corresponding to coherent quasiparticle-based transport in the Fermi liquid state. At high temperatures, the shear viscosity shows significant deviation from Fermi liquid state behavior. This corresponds to crossover from coherent quasiparticle-based transport to incoherent transport (the "bad metal"). With increasing interaction strength U, the shear viscosity becomes less than conjectured quantum limits of shear viscosity, of the order of $n\hbar$. Finally, we considered the scaled dimensionless ratio between shear viscosity and entropy density. This ratio in the Hubbard model depends on the energy scale t^*, length scale a, and the free-fermion mass m. This is in contrast to the universal limit $\frac{\hbar}{4\pi k_B}$ predicted by Kovtun, Son, and Starinets using the AdS/CFT correspondence in a conformally symmetric field theory model. For ^{3}He parameters, the ratio is above the universal bound but for parameters appropriate for electronic lattice systems, such as cuprate and organic metals, this bound is found to be strongly violated, in the bad metal regime near the Mott metal-insulator transition. We hope that our results will stimulate experimental measurements of the shear viscosity in bad metals.

ACKNOWLEDGMENTS

We would like to acknowledge useful discussions with R. Adhikari, J. Analytis, A. Andreev, G. Baskaran, A. Bulgac, V. Dobrosavljevic, S. Hartnoll, S. Kalyan Rama, M. Laad, R. Mann, B. Sathiapalan, T. Schäfer, B. Spivak, D. Tanaskovic, D. Vollhardt, J. Vucicevic, and G. Wlazlowski. We thank Y. Huang for providing data from Ref. [2]. We thank M. Kollar for drawing our attention to analytical derivation of Eq. (38).

This work was supported by a Discovery Project grant from the Australian Research Council.

APPENDIX: TRANSPORT DENSITY OF STATES FOR SHEAR VISCOSITY

In the limit $d \to \infty$, the viscosity will involve the following transport function:

$$\Theta_{xy}(\epsilon) = m^2 \sum_{\mathbf{k}} v_x^2 v_y^2 \delta(\epsilon - \epsilon_{\mathbf{k}}). \tag{A1}$$

For a d-dimensional hypercubic lattice

$$\Theta_{xy}(\epsilon) = \frac{m^2 (2t)^4 a^4}{\hbar^4} \sum_{\mathbf{k}} \sin^2(k_x) \sin^2(k_y) \delta(\epsilon - \epsilon_{\mathbf{k}}). \tag{A2}$$

To evaluate this, we first we define the Fourier transform

$$\begin{aligned} Y(\omega) &= \int_{-\infty}^{+\infty} \Theta_{xy}(\epsilon) e^{-i\omega\epsilon} d\epsilon \\ &= \gamma^2 (2t)^4 \sum_{\mathbf{k}} \sin^2(k_1) \sin^2(k_2) \prod_{\alpha=1}^{d} e^{i2t\omega \cos(k_\alpha)} \\ &= \gamma^2 (2t)^4 J_0^{d-2}(2t\omega) \left[\frac{J_1(2t\omega)}{2t\omega} \right]^2 \\ &= \frac{(2t\gamma)^2}{\omega^2} J_0^{d-2}(2t\omega) [J_1(2t\omega)]^2, \end{aligned} \tag{A3}$$

where $\gamma \equiv \frac{ma^2}{\hbar^2}$.

Using relations for Bessel functions

$$\begin{aligned} &[J_0(2t\omega)]^{d-2} [J_1(2t\omega)]^2 \\ &= \frac{1}{(2t)^2 d(d-1)} \frac{d^2 J_0^d(2t\omega)}{d\omega^2} \\ &\quad + \frac{1}{d-1} J_0^d(2t\omega) - \frac{1}{2t(d-1)} \frac{1}{\omega} [J_0(2t\omega)]^{d-1} J_1(2t\omega) \end{aligned} \tag{A4}$$

we can rewrite $Y(\omega)$ as

$$\begin{aligned} Y(\omega) &= \frac{\gamma^2}{d(d-1)} \frac{1}{\omega^2} \frac{d^2 J_0(2t\omega)}{d\omega^2} + \frac{(2t\gamma)^2}{(d-1)} \frac{1}{\omega^2} J_0^d(2t\omega) \\ &\quad - \frac{2t\gamma^2}{(d-1)} \frac{1}{\omega^3} [J_0(2t\omega)]^{d-1} J_1(2t\omega) \\ &\equiv Y_1(\omega) + Y_2(\omega) + Y_3(\omega). \end{aligned} \tag{A5}$$

We can Fourier transform back to calculate $\Theta_{xy}(\epsilon)$ as

$$\Theta_{xy}(\epsilon) = \frac{1}{2\pi} \int_{-\infty}^{+\infty} Y(\omega) e^{i\omega\epsilon} d\omega. \tag{A6}$$

Using the convolution theorem, we can easily show that each term of $Y(\omega)$ has the following form:

$$\Theta_{xy}^{(\alpha)}(\epsilon) = \int_{-\infty}^{+\infty} F_\alpha(\epsilon - z) G_\alpha(z) dz, \quad \alpha = 1, \ldots, 3 \tag{A7}$$

where

$$\begin{aligned} F_\alpha(\epsilon) &= \frac{1}{2\pi} \int_{-\infty}^{+\infty} \tilde{F}_\alpha(\omega) e^{i\omega\epsilon} d\omega, \\ G_\alpha(\epsilon) &= \frac{1}{2\pi} \int_{-\infty}^{+\infty} \tilde{G}_\alpha(\omega) e^{i\omega\epsilon} d\omega, \end{aligned} \tag{A8}$$

and $Y_\alpha(\omega) = \tilde{F}_\alpha(\omega) \tilde{G}_\alpha(\omega)$.

For the first term

$$\begin{aligned} F_\alpha(\epsilon) &= \frac{1}{2\pi} \int_{-\infty}^{+\infty} \frac{1}{\omega^2} e^{i\omega\epsilon} d\omega \\ &= \frac{1}{2\pi} \cdot \pi i \cdot i\epsilon \ \mathrm{sgn}(\epsilon) = -\frac{\epsilon}{2} \mathrm{sgn}(\epsilon), \end{aligned} \tag{A9}$$

$$\begin{aligned} G_\alpha(\epsilon) &= \frac{1}{2\pi} \int_{-\infty}^{+\infty} \frac{d^2 [J_0(2t\omega)]^d}{d\omega^2} e^{i\omega\epsilon} d\omega \\ &= -\epsilon^2 N_0(\epsilon), \end{aligned} \tag{A10}$$

where we have used

$$\begin{aligned} \frac{d[J_0(2t\omega)]^d}{d\omega} e^{i\omega\epsilon} \Big|_{-\infty}^{+\infty} &= 0, \\ [J_0(2t\omega)]^d e^{i\omega\epsilon} \big|_{-\infty}^{+\infty} &= 0. \end{aligned} \tag{A11}$$

Finally, we get

$$\begin{aligned} \Theta_{xy}^{(1)}(\epsilon) &= \frac{\gamma^2 \epsilon}{d(d-1)} \int_{-\infty}^{\epsilon} z^2 N_0(z) dz - \frac{(2t\gamma)^2 \epsilon}{4(d-1)} \\ &\quad - \frac{\gamma^2}{d(d-1)} \int_{-\infty}^{\epsilon} z^3 N_0(z) dz, \end{aligned} \tag{A12}$$

where we have used $\int_{-\infty}^{+\infty} z^2 N_0(z) dz = \sum_{\mathbf{k}} \epsilon_{\mathbf{k}}^2 = 2t^2 d$ and $\int_{-\infty}^{+\infty} z^3 N_0(z) dz = 0$.

A similar exercise for the second term will give

$$\begin{aligned} \Theta_{xy}^{(2)}(\epsilon) &= -\frac{(2t\gamma)^2 \epsilon}{(d-1)} \int_{-\infty}^{\epsilon} N_0(z) dz + \frac{(2t\gamma)^2 \epsilon}{2(d-1)} \\ &\quad + \frac{(2t\gamma)^2}{(d-1)} \int_{-\infty}^{\epsilon} z N_0(z) dz. \end{aligned} \tag{A13}$$

For the third term we have

$$\begin{aligned} F_3(\epsilon) &= \frac{1}{2\pi} \int_{-\infty}^{+\infty} \frac{1}{\omega^3} e^{i\omega\epsilon} d\omega \\ &= \lim_{\omega \to 0} \frac{1}{2\pi} \pi i \frac{1}{2!} \frac{d^2}{d\omega^2} [e^{i\omega\epsilon}] \mathrm{sgn}(\epsilon) \\ &= -i \frac{\epsilon^2}{4} \mathrm{sgn}(\epsilon) \end{aligned} \tag{A14}$$

and

$$\begin{aligned} G_3(\epsilon) &= -\frac{1}{2\pi} \frac{2t\gamma^2}{(d-1)} \int_{-\infty}^{+\infty} [J_0(2t\omega)]^{d-1} J_1(2t\omega) d\omega \\ &= \frac{1}{2\pi} \frac{\gamma^2}{d(d-1)} \int_{-\infty}^{+\infty} \frac{d[J_0(2t\omega)]^d}{d\omega} d\omega \\ &= -i \frac{\gamma^2}{d(d-1)} \epsilon N_0(\epsilon). \end{aligned} \tag{A15}$$

Finally, we have

$$\Theta^{(3)}_{xy}(\epsilon) = -\frac{\gamma^2\epsilon^2}{2d(d-1)}\int_{-\infty}^{\epsilon} zN_0(z)dz - \frac{(2t\gamma)^2\epsilon}{4(d-1)} + \frac{\gamma^2\epsilon}{d(d-1)}\int_{-\infty}^{\epsilon} z^2N_0(z)dz - \frac{\gamma^2}{2d(d-1)}\int_{-\infty}^{\epsilon} z^3N_0(z)dz. \quad \text{(A16)}$$

Collecting and rearranging all the terms, we obtain Eq. (30).

[1] A. B. Bhatia, *Ultrasonic Absorption: An Introduction to the Theory of Sound Absorption and Dispersion in Gases, Liquids and Solids* (Oxford University Press, Oxford, UK, 1967), p. 54.
[2] Y. Huang, Q. Yu, Q. Chen, and R. Wang, Cryogenics **52**, 538 (2012).
[3] M. S. Steinberg, Phys. Rev. **109**, 1486 (1958).
[4] H. Eyring, J. Chem. Phys. **4**, 236 (1936).
[5] J. Merino and R. H. McKenzie, Phys. Rev. B **61**, 7996 (2000).
[6] N. E. Hussey, K. Takenaka, and H. Takagi, Philos. Mag. **84**, 2847 (2004).
[7] O. Gunnarsson, M. Calandra, and J. E. Han, Rev. Mod. Phys. **75**, 1085 (2003).
[8] S. Sachdev and M. Müller, J. Phys.: Condens. Matter **21**, 164216 (2009).
[9] T. Faulkner, N. Iqbal, H. Liu, J. McGreevy, and D. Vegh, Science **329**, 1043 (2010).
[10] H. Liu, Phys. Today **65**(6), 68 (2012).
[11] S. A. Hartnoll, Nat. Phys. **11**, 54 (2014).
[12] R. A. Davison, K. Schalm, and J. Zaanen, Phys. Rev. B **89**, 245116 (2014).
[13] J. M. Maldacena, Adv. Theor. Math. Phys. **2**, 231 (1998).
[14] P. K. Kovtun, D. T. Son, and A. O. Starinets, Phys. Rev. Lett. **94**, 111601 (2005).
[15] E. Shuryak, Prog. Part. Nucl. Phys. **53**, 273 (2004).
[16] C. Cao, E. Elliott, J. Joseph, H. Wu, J. Petricka, T. Schäfer, and J. E. Thomas, Science **331**, 58 (2011).
[17] M. Müller, J. Schmalian, and L. Fritz, Phys. Rev. Lett. **103**, 025301 (2009).
[18] C. Chafin and T. Schäfer, Phys. Rev. A **87**, 023629 (2013).
[19] G. Wlazłowski, P. Magierski, A. Bulgac, and K. J. Roche, Phys. Rev. A **88**, 013639 (2013).
[20] E. Elliott, J. A. Joseph, and J. E. Thomas, Phys. Rev. Lett. **113**, 020406 (2014).
[21] G. Wlazlowski, W. Quan, and A. Bulgac, arXiv:1504.02560v2.
[22] T. D. Cohen, Phys. Rev. Lett. **99**, 021602 (2007); A. Sinha and R. C. Myers, Nucl. Phys. A **830**, 295c (2009); S. Cremonini, Mod. Phys. Lett. B **25**, 1867 (2011).
[23] N. Pakhira and R. H. McKenzie, Phys. Rev. B **91**, 075124 (2015).
[24] T. Schäfer, Annu. Rev. Nucl. Part. Sci. **64**, 125 (2014).
[25] G. M. Bruun and H. Smith, Phys. Rev. A **75**, 043612 (2007).
[26] E. Taylor and M. Randeria, Phys. Rev. A **81**, 053610 (2010).
[27] N. Ashcroft and N. Mermin, *Solid State Physics* (Saunders College, Philadelphia, 1976).
[28] F. S. Khan and P. B. Allen, Phys. Rev. B **29**, 3341 (1984).
[29] F. S. Khan and P. B. Allen, Phys. Rev. B **35**, 1002 (1987).
[30] K. Rah and B. C. Eu, Phys. Rev. E **60**, 4105 (1999).
[31] T. Enss, R. Haussmann, and W. Zwerger, Ann. Phys. (NY) **326**, 770 (2011).
[32] W. Metzner and D. Vollhardt, Phys. Rev. Lett. **62**, 324 (1989).
[33] A. Georges, G. Kotliar, W. Krauth, and M. J. Rozenberg, Rev. Mod. Phys. **68**, 13 (1996).
[34] P. Limelette, P. Wzietek, S. Florens, A. Georges, T. A. Costi, C. Pasquier, D. Jérome, C. Mézière, and P. Batail, Phys. Rev. Lett. **91**, 016401 (2003).
[35] J. Merino, M. Dumm, N. Drichko, M. Dressel, and R. H. McKenzie, Phys. Rev. Lett. **100**, 086404 (2008).
[36] B. J. Powell and R. H. McKenzie, Rep. Prog. Phys. **74**, 056501 (2011).
[37] G. Kotliar, S. Y. Savrasov, K. Haule, V. S. Oudovenko, O. Parcollet, and C. A. Marianetti, Rev. Mod. Phys. **78**, 865 (2006).
[38] X. Y. Zhang, M. J. Rozenberg, and G. Kotliar, Phys. Rev. Lett. **70**, 1666 (1993).
[39] H. Kajueter and G. Kotliar, Phys. Rev. Lett. **77**, 131 (1996).
[40] R. Bulla, Phys. Rev. Lett. **83**, 136 (1999).
[41] H. Terletska, J. Vučičević, D. Tanasković, and V. Dobrosavljević, Phys. Rev. Lett. **107**, 026401 (2011).
[42] S. Sachdev, Phys. Rev. Lett. **105**, 151602 (2010).
[43] A. Khurana, Phys. Rev. Lett. **64**, 1990 (1990).
[44] L.-F. Arsenault and A.-M. S. Tremblay, Phys. Rev. B **88**, 205109 (2013).
[45] G. Aarts and J. M. Martinez Resco, J. High Energy Phys. 04 (2002) 053.
[46] D. S. Novikov, arXiv:cond-mat/0603184.
[47] N. Lin, E. Gull, and A. J. Millis, Phys. Rev. B **80**, 161105 (2009).
[48] D. Bergeron, V. Hankevych, B. Kyung, and A.-M. S. Tremblay, Phys. Rev. B **84**, 085128 (2011).
[49] E. Economou, *Green's Functions in Quantum Physics* (Springer, Berlin, 2010).
[50] A. Georges and W. Krauth, Phys. Rev. B **48**, 7167 (1993).
[51] T. Pruschke, D. L. Cox, and M. Jarrell, Phys. Rev. B **47**, 3553 (1993).
[52] G. Moeller, V. Dobrosavljević, and A. E. Ruckenstein, Phys. Rev. B **59**, 6846 (1999).
[53] D. Vollhardt, Rev. Mod. Phys. **56**, 99 (1984).
[54] D. Vollhardt, P. Wölfle, and P. W. Anderson, Phys. Rev. B **35**, 6703 (1987).
[55] K. Seiler, C. Gros, T. Rice, K. Ueda, and D. Vollhardt, J. Low Temp. Phys. **64**, 195 (1986).
[56] A. Georges and L. Laloux, Mod. Phys. Lett. B **11**, 913 (1997).
[57] D. Vollhardt, Phys. Rev. Lett. **78**, 1307 (1997).
[58] J. C. Wheatley, Rev. Mod. Phys. **47**, 415 (1975).
[59] A. Toschi, M. Capone, C. Castellani, and K. Held, Phys. Rev. Lett. **102**, 076402 (2009).
[60] J. Vucicevic (private communication).
[61] M. Platé *et al.*, Phys. Rev. Lett. **95**, 077001 (2005).
[62] G. K. Straub and W. A. Harrison, Phys. Rev. B **31**, 7668 (1985).
[63] J. D. Rameau, T. J. Reber, H.-B. Yang, S. Akhanjee, G. D. Gu, P. D. Johnson, and S. Campbell, Phys. Rev. B **90**, 134509 (2014).

[64] W. P. Mason, Phys. Rev. **97**, 557 (1955).
[65] E. Lax, Phys. Rev. **115**, 1591 (1959).
[66] A. Pippard, Philos. Mag. **46**, 1104 (1955).
[67] B. Batlogg, D. J. Bishop, B. Golding, E. Bucher, J. Hufnagl, Z. Fisk, J. L. Smith, and H. R. Ott, Phys. Rev. B **33**, 5906(R) (1986).
[68] A. Migliori and J. L. Sarrao, *Resonant Ultrasound Spectroscopy: Applications to Physics, Materials Measurements, and Nondestructive Evaluation* (Wiley, New York, 1997).
[69] R. G. Leisure and F. A. Willis, J. Phys.: Condens. Matter **9**, 6001 (1997).
[70] A. Migliori and J. D. Maynard, Rev. Sci. Instrum. **76**, 121301 (2005).
[71] J. L. Sarrao, D. Mandrus, A. Migliori, Z. Fisk, and E. Bucher, Phys. B (Amsterdam) **199-200**, 478 (1994).
[72] M. A. Carpenter, C. J. Howard, R. E. A. McKnight, A. Migliori, J. B. Betts, and V. R. Fanelli, Phys. Rev. B **82**, 134123 (2010).
[73] A. Shekhter, B. J. Ramshaw, R. Liang, W. N. Hardy, D. A. Bonn, F. F. Balakirev, R. D. McDonald, J. B. Betts, S. C. Riggs, and A. Migliori, Nature (London) **498**, 75 (2013).
[74] D. Forcella, J. Zaanen, D. Valentinis, and D. van der Marel, Phys. Rev. B **90**, 035143 (2014).
[75] A. Tomadin, G. Vignale, and M. Polini, Phys. Rev. Lett. **113**, 235901 (2014).
[76] L. Levitov and G. Falkovich, arXiv:1508.00836.
[77] I. Torre, A. Tomadin, A. K. Geim, and M. Polini, arXiv:1508.00363.